

Wake impact on aerodynamic characteristics of horizontal axis wind turbine under yawed flow conditions

Hakjin Lee and Duck-Joo Lee*

Korea Advanced Institute of Science and Technology (KAIST), Daejeon 34141, Republic of Korea

Abstract

Wind turbines spend most of time in complex and unsteady environment, such as yawed flow, atmospheric wind turbulence, wind shear, and gust. Under yawed flow condition, velocity component parallel to the rotating plane causes a development of skewed wake structure, thus leading to an azimuthal variation in the aerodynamic loads on wind turbine blades. Moreover, the trailing and shed wake vortices unequally expand, and a strong wake interaction between the hub and tip vortices, and the asymmetrical velocity deficit around the rotor area occur. In the present study, the impacts of the skewed wake on the unsteady aerodynamic behavior around rotor blade were numerically investigated and a wake deflection mechanism was discussed in detail. For this purpose, the nonlinear vortex lattice method (NVLM) coupling with a time-accurate vortex particle method (VPM) was used. A numerical simulation on the NREL Phase VI wind turbine model, exposed to a low wind speed with different yaw angles, was carried out and predicted results were compared against measurements. Comparison results showed that the aerodynamic loads can be accurately calculated, even for highly yawed flow conditions and complex wake dynamics can be clearly observed.

Keywords: Wind turbine aerodynamics; Wind turbine wake; Yaw misalignment; Skewed wake structure; Vortex particle method; Nonlinear vortex lattice method

*Corresponding author. KAIST, 291 Daehak-ro, Yuseng-gu, Daejeon 34141, Republic of Korea.

Tel.: +82-42-350-3716; fax: +82-42-350-3710; E-mail: djlee@kaist.ac.kr, djlee@kaist.edu

1. Introduction

Wind turbines are subjected to various unsteady and transient environment such as yaw misalignment, atmospheric turbulence, wind shear flow, and gusts. In particular, they operate a considerable time under the yawed flow condition as the direction of the wind is not parallel to the rotating axis of wind turbine. When yaw misalignment is present, the wind turbine blades experience unsteady aerodynamic behavior and loads with respect to the radial and azimuthal position. These may have a negative impact on the fatigue lifetime of the rotor blades and may cause structural damage to the wind turbine's components as well as a significant reduction in the quality of power generation. The necessity of an in-depth understanding of yaw aerodynamics has recently been recognized as an intentional yaw misalignment of upstream wind turbines are emerging as an active control strategy for alleviating the power loss of downstream wind turbines. Although the power output generated from an upstream wind turbine is slightly reduced due to yaw error, an unfavorable wake impingement can be effectively mitigated at the subsequent wind turbines by artificially developing a deflected wake structure [1, 2]. Hence, wind turbines placed at the downstream can potentially harvest more energy from the incoming flow. This is called the wake steering technique, which can improve the overall wind farm efficiency and help to minimize the fatigue loads acting on the downstream wind turbine's components. Therefore, a study on the propagation of the deflected wake and its unsteady characteristics is becoming more prominent in the area of wind turbines.

Under yawed flow conditions, the wind turbine blades suffer from a cycle-to-cycle variation in aerodynamic loads. This is mainly attributed to the advancing and retreating blade effect and skewed wake effect. Of the two effects, the former becomes more dominant at higher wind speed. It can induce the dynamic stall on the rotor blades, after which they will experience a periodic variation in the angle of attack with a large amplitude, in particular at the inboard section. As a result, the hysteresis loop of the aerodynamic loads may cause an extreme loading on the rotor blade and, therefore, structural damage to the wind turbine system. In contrast, the skewed wake structure plays a more important role in the wind turbine aerodynamics at low wind speed. It is found that the complicated vortex structures in the deflected wake are responsible for the asymmetrical distribution of the induced velocity and aerodynamic loads on the rotor plane. In addition, the skewed wake structure has a profound effect on the unsteady aerodynamic behavior of the rotor blade from hub to tip regions. However, predicting the evolution of deflected wake geometry, and its influence on the aerodynamic characteristics around the rotor blades, still remains a challenge because of the complexity of the skewed wake structure.

Experimental studies on the wind turbine wake using optimal equipment were conducted to measure the tip vortex trajectories and wake deflection by Grant et al. [3] and Grant and Parkin [4]. The measurements on the wake geometries with various operating conditions including tip speed ratio, tip pitch angle, and yaw angles, were also carried out by Vermmer [5] and Haans et al. [6]. Using the flow visualization method, the wake flow behind the yawed rotor configuration was measured to investigate the effect of the incoming atmospheric boundary-layer (ABL) and the turbulent inflow conditions on the wake characteristics by Bastankhah and Porté-Agel [7], and Bartl and Sætran [8], respectively. Howland et al. [9] observed the curled wake morphology using hot wire anemometry and a Pitot-static probe, and discussed the transient wake behaviors in detail. Extensive measurements on wind turbines under yawed flow conditions, to provide high quality data regarding blade aerodynamic loading and flow fields around wind turbines, were reported by Schepers et al. [10, 11]. Furthermore, numerical works have also been devoted to analyzing yaw aerodynamics and flow characteristics. Schepers [12] developed an improved engineering model based on inflow measurements for numerically predicting the aerodynamic loads of the rotor blade at yawed conditions. The aerodynamic performance and time-varying blade loading of wind turbines under yawed flow conditions were evaluated and compared against the experimental results using various numerical methods by Ryu et al. [13], Dueque et al. [14], Shen et al. [15], Tongchitpakdee et al. [16], and Yu et al. [17]. However, many studies have focused mainly on accurately predicting the aerodynamic performance of yawed wind turbines, hence they did not pay much attention to unsteady wake characteristics.

The main objective of the present study is to numerically investigate the effect of skewed wake structures on the unsteady aerodynamic behaviors of the rotor blade and reveal the wake deflection mechanism. For this paper, the numerical simulation on the NREL Phase VI wind turbine model, exposed to a low wind speed with different yaw angles, is carried out and the occurring aerodynamic characteristics are discussed in detail. For these purposes, the nonlinear vortex lattice method (NVLM), which is tightly coupled with vortex lattice method (VLM), airfoil look-up table, and vortex strength correction, is used for calculating aerodynamic loads on the wind turbine blades. In addition, the vortex particle method (VPM) is adopted to model the shedding rotor wake and represent a vorticity field behind the rotor blades. The radial distributions of the aerodynamic loads computed by NVLM are compared against the experimental data, and the impacts of skewed wake structure on the induced velocity and aerodynamic loads on the wind turbine blade are investigated. Moreover, the development of skewed wake structure and transient flow field in

the downstream are observed. Discussion in the current work can help to achieve a better understanding of the wake-induced phenomena and evolving pattern of the deflected wake.

2. Numerical method

2.1 Aerodynamic model

Many studies have been devoted to developing aerodynamic models for wind turbine applications that can predict the aerodynamic loads acting on the rotor blades and describe an underlying flow field around wind turbines. The most current comprehensive wind turbine analysis codes adopt the blade element momentum (BEM) theory. Although the BEM is computationally efficient, it is only able to capture the quasi-steady solutions owing to the inherent assumption. Furthermore, the BEM cannot take into account the effects of the radial flow in the spanwise direction because it ignores the mutual aerodynamic interactions between adjacent blade elements. The accuracy of BEM results relies greatly on the various correction models, such as the tip loss model, skewed wake model, and dynamic inflow model. On the other hand, computational fluid dynamics (CFD) methods are the most high-fidelity and expensive way of analyzing the flow field around wind turbines. However, CFD methods intrinsically suffer from a grid-induced dissipation error caused by the numerical discretization over the flow field. An excessive dissipation error may incur the considerable under-prediction in the intensity of tip vortex and a rapid decay of the vorticity structure downstream. Therefore, the complicated wake behavior, such as wake-wake interaction or skewed wake structure, could not be accurately described. To resolve mentioned numerical problems, a finer grid resolution is required downstream as well as near the rotor blade. However, this will lead to extremely high computational costs and resources. In the case of wind turbines, vortex methods would be a better approach to predict both the aerodynamic performance and wake structures, because wind turbine mostly operates at low wind and rotational speeds, which can be regarded as the incompressible flow. Moreover, the vorticity field behind the rotor blade can be described without the numerical dissipation error. Vortex methods yield more accurate solutions than BEM methods and require much less computing resources than CFD methods.

In the current study, the nonlinear vortex lattice method (NVLM) was employed to investigate the impacts of skewed wake geometry on wind turbine yaw aerodynamics. NVLM has been suggested to overcome the inherent shortcomings of the classical vortex lattice method (VLM). This is possible by incorporating the airfoil look-up table and iterative vortex strength correction. The sectional aerodynamic loads were evaluated through the look-up table as

a function of local inflow velocity and effective angle of attack at the control points where they are placed at a half chord of the camber line. In addition, the computed sectional lift forces were also used to correct the sectional circulation strength calculated from the VLM. According to the Kutta condition, the corrected circulation strength at the current time step will be employed to model the wake at the next time step. A proper location of the control points for NVLM can be determined by applying the zero normal flow condition on the two-dimensional camber airfoil surface. To find the numerical position of the control points, the camber airfoil was modeled by M number of point vortex elements with a strength of circulation Γ_i in the chordwise direction. Eq. (1) shows the induced velocity at an arbitrary control point due to discrete vortex elements, while Eq. (2) indicates the normal component of the freestream at the arbitrary control point with a small angle assumption. Here i implies the index in the chordwise direction. x_{cp} and y_{cp} are the coordinates of the control point, x_i and y_i are the coordinates of the i -th point vortex, and r_i is the distance between the control point and the i -th point vortex. The final equation for finding an unknown location of a control point can be derived by combining Eq. (1) and (2) with the relation between the expression for the freestream velocity of the Kutta-Joukowski theorem and thin airfoil theory. The derived equation was numerically solved using the root-finding approach.

$$V_{cp} = \sum_{i=1}^M \frac{\Gamma_i}{2\pi r_i} = \sum_{i=1}^M \frac{\Gamma_i}{2\pi \sqrt{(x_{cp} - x_i)^2 + (y_{cp} - y_i)^2}} \quad \text{Eq. (1)}$$

$$V_{\infty,n} = V_{\infty} \sin\left(\alpha + \tan^{-1}\left(-\frac{dy_c}{dx}\right)\right) \approx V_{\infty} \left(\alpha - \frac{dy_c}{dx}\right) \quad \text{Eq. (2)}$$

To make use of the aerodynamic coefficients from the airfoil table, the inflow velocity ($\mathbf{V}_{\text{inflow}}$) and effective angle of attack (α_{eff}) should be evaluated at each blade section, as shown in Eq. (3) and (4). Here \mathbf{V}_{∞} is the free stream velocity, $\boldsymbol{\Omega} \times \mathbf{r}$ is the rotor rotational velocity, $\mathbf{V}_{\text{ind,bound}}$ is the self-induced velocity, and $\mathbf{V}_{\text{ind,wake}}$ is the wake-induced velocity. In addition, α_{inflow} is the local inflow angle and ϕ_{geo} is the local geometric pitch angle including local twist angle and collective pitch angle at each blade section. \mathbf{a}_1 and \mathbf{a}_3 are the unit vectors along the tangential and normal to the rotating plane, respectively.

$$\mathbf{V}_{\text{inflow}} = \mathbf{V}_{\infty} - \boldsymbol{\Omega} \times \mathbf{r} + \mathbf{V}_{\text{ind,bound}} + \mathbf{V}_{\text{ind,wake}} \quad \text{Eq. (3)}$$

$$\alpha_{\text{eff}} = \alpha_{\text{inflow}} - \phi_{\text{geo}} = \tan^{-1} \left(\frac{\mathbf{V}_{\text{inflow}} \cdot \mathbf{a}_3}{\mathbf{V}_{\text{inflow}} \cdot \mathbf{a}_1} \right) - \phi_{\text{geo}} \quad \text{Eq. (4)}$$

Consequently, NVLM can consider the thickness, viscous effects, and the nonlinear aerodynamic characteristics occurring at the high angle of attack or low Reynold number. Compared to the lifting line method (LLM), it is also able to accurately represent the various geometries of wind turbine blades, including the curvature, camber, and swept angle, by using chordwise and spanwise distribution of vortex ring elements. The model accuracy of NVLM has been validated in our research papers [18, 19]. NVLM is also incorporated in a vortex particle method (VPM) for modeling the wind turbine wake shed from the trailing edge of the blades. A detailed description of the vortex particle method is discussed in the following section.

2.2 Wake model

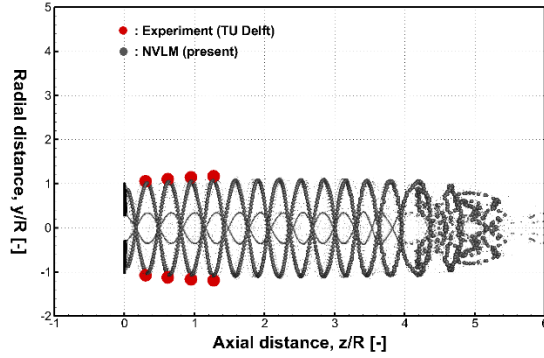
It is important to accurately understand and predict the wind turbine wake because its structure is one of the most critical factors in determining wind turbine performance. In the vortex method, a grid-free Lagrangian formulation is used for wake modeling that does not involve an artificial dissipation error. Hence, it can provide a physically meaningful solution for simulating wake transportation, and can preserve the concentrated vorticity without an undesirable numerical error. In the current study, the rotor wake is shed from the whole span of the wind turbine blade, and its structure is represented by vortex particles, rather than vortex filaments. The vortex filament is modeled as concentrated vortices along a segment with a singularity at the center, while the vortex particle is modeled as concentrated vortices within a certain volume. Therefore, the vortex particles can be regarded as a small section of a vortex tube. The vortex particles do not necessarily need to maintain connectivity between adjacent particles because they are independently transported during the time-marching step. This property is especially useful for investigating the effect of wake-wake or wake-body interaction. It has been proved that the vortex particle method (VPM) has the capability to model complicated wake structures of helicopter rotor wake [20], rotor-fuselage wake interaction [21], and main-tail rotors wake interaction [22]. The vorticity field in the wake is represented by a number of vortex particles as follows:

$$\boldsymbol{\omega}(\mathbf{x}, t) = \sum_{i=1}^p \boldsymbol{\alpha}_i(t) \zeta_{\sigma}(\mathbf{x} - \mathbf{x}_i(t)) = \sum_{i=1}^p V_i \boldsymbol{\omega}_i(\mathbf{x}_i, t) \zeta_{\sigma}(\mathbf{x} - \mathbf{x}_i(t)) \quad \text{Eq. (5)}$$

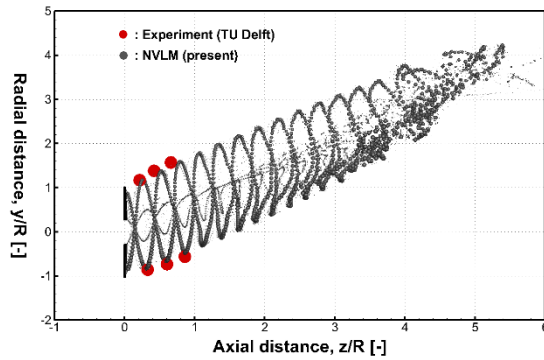
$$\zeta_{\sigma}(\mathbf{r}) = \frac{1}{\sigma_3} \frac{15}{8\pi} \left[\left(\frac{|\mathbf{r}|}{\sigma} \right)^2 + 1 \right]^{-7/2} \quad \text{Eq. (6)}$$

where $\boldsymbol{\omega}(\mathbf{x}, t)$ is the vorticity in the wake, $\boldsymbol{\alpha}_i(t)$ is a strength vector, and V_i is the volume of the i -th vortex particle. \mathbf{x} is the position vector of an arbitrary point in the field, \mathbf{x}_i is the position vector of the i -th vortex particle, and \mathbf{r} is the position vector between \mathbf{x} and \mathbf{x}_i . p is the number of vortex particles distributed in the field. σ is a smoothing radius and $\zeta_{\sigma}(\rho)$ is the three-dimensional regularization function or smoothing function which is needed to avoid a singularity problem. In the present study, the value of the smoothing radius is equal to a core radius of a vortex particle, and the higher order algebraic smoothing function proposed by Winckelmans and Leonard is employed to represent the vorticity distribution near the vortex particle [23]. The strength of the recently shed vortex particles can be determined by imposing the Kutta condition at the vortex elements placed at the trailing edge of the rotor blade. Vortex particles are allowed to mutually interact with each other, freely distort, and naturally transport downstream with local convection velocity. A numerical time integration method is required to update their position at each time step, and it plays an important role in the accuracy and stability of the wake solution. In the present research, the second order Runge-Kutta method was used.

Comparing tip vortex trajectories in terms of the radial and axial positions is a practical way for validating the wake models. Wake geometries of TU Delft wind turbine model under axial and yawed flow conditions were measured at an open jet tunnel in the Delft University of Technology (DUT) using a flow visualization technique [6]. Tip vortex trajectories with respect to time were predicted by the present method, and compared with experiments. The comparison results showed that the radial and axial positions of the wake structures represented by vortex particles are well matched with the measured data, as shown in Fig. 1. It was found that the vortex particle method (VPM) is capable of accurately modeling the wind turbine wake.



(a) $\lambda = 8, \theta_{tip} = 2^\circ, \beta = 0^\circ$



(b) $\lambda = 8, \theta_{tip} = 2^\circ, \beta = -30^\circ$

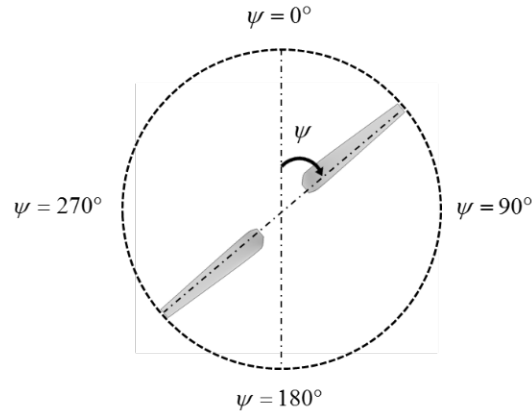
Fig. 1. Tip vortex trajectories of TU Delft wind turbine model under axial and yawed conditions

3. Results and discussion

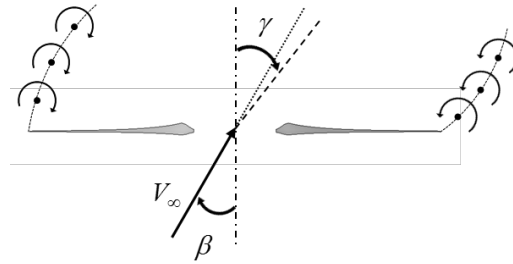
3.1 Wind turbine model

A notable measurement on the NREL Phase VI wind turbine was conducted to obtain the comprehensive high-quality database at the NASA-Ames wind tunnel facilities in 2000 [24]. In this experiment, various yaw angles and wind speeds corresponding to the attached and stalled flow conditions were considered, while the rotational speed has remained constant at 72 rpm. They provided extensive data including surface pressure, distributions of the aerodynamic loads in the radial direction, and integrated wind turbine performance. These measurements were widely employed to validate the accuracy of aerodynamic models for wind turbines, such as the BEM, vortex methods, and CFD methods. NREL Phase VI wind turbine consists of two-bladed rotors without hub tilt, coning, and prebend angles. The rotor blade is composed of S809 airfoil and has a tapered-twisted configuration. The diameter of the rotor blades

is about 10m, and the tip pitch angle is 3° . As aforementioned, the main focus of the present study is to improve our understanding of the unsteady wake structures and wake-wake interaction phenomenon caused by yaw misalignment. Therefore, low wind speed condition (7m/s) with different yaw angles (0° , 30° , 45° , and 60°) have been considered to investigate the effects of the skewed wake structure on the aerodynamic characteristics of wind turbine blades and flow field in the downstream. A wind profile is assumed to be uniform and homogeneous.



(a) Front view



(b) Top view

Fig. 2. Definition of azimuth and yaw angles

The positive azimuth and yaw angles are defined according to Fig. 2. The rotor blades rotate in a clockwise direction, as viewed from upstream, and an azimuth angle of zero indicates the blade pointing vertically upward. Under yawed flow conditions, the upper half of the rotor disc ($0^\circ \leq \psi \leq 90^\circ$ and $270^\circ \leq \psi \leq 360^\circ$) corresponds to the retreating side, while the lower half of the rotor disc ($90^\circ \leq \psi \leq 270^\circ$) corresponds to the advancing side. In

addition, the positive yaw misalignment induces the downwind and upwind sides at azimuth angles of 90° and 270° , respectively.

The NREL rotor blade was discretized using 20 (chordwise) \times 40 (spanwise) quadrilateral vortex ring elements with a grid clustering near the inboard and outboard locations, and the rotor wake was modeled by Lagrangian-based vortex particles. The simulation was conducted for a total of 20 revolutions, including 1 revolution of slow-starting rotation to prevent a numerical instability problem in the wake solution, mainly associated with an impulsive rotation, and a discretization of the time step $\Delta\psi = 5^\circ$ was used.

3.2 Averaged aerodynamic forces

The average normal and tangential forces over one revolution were computed at the wind speed of 7 m/s and yaw angles of 0° , 30° , 45° , and 60° , and compared with the NREL measurement data [24] and the numerical results were computed by LLM [15] and RANS [16], as shown in the schematic in Fig. 3 and Fig. 4, respectively. Compared to other methods, NVLM can yield the most accurate prediction in the aerodynamic loads from the inboard to outboard regions for all yaw angles. It is noticeable that the radial distributions of the normal and tangential forces computed by NVLM are in quite good agreement with the measured data, even for highly yawed flow conditions. Although LLM tends to slightly underestimate the averaged normal force at highly yawed conditions, all numerical results for predicting normal force distributions generally agree well against experiments, as indicated in Fig. 3. However, the significant under-prediction in the tangential forces can be observed in the LLM and RANS results. These disparities had become more pronounced, especially at the inboard region, as the yaw angle increased. Yawed flow induces a strong spanwise velocity and momentum that deflect the wake geometry of the wind turbine in a skewed direction. Because of the skewed wake structures, the complicated and unsteady wake behavior, such as the wake-wake interaction between the hub and tip vortices, occurs. These phenomena become more severe and significantly affect the aerodynamic loads acting on the wind turbine blades as the yaw angle increases. However, the RANS simulation is not able to preserve the intensity of the vortices and wake structures to the far downstream because of a grid-induced dissipation error. Hence, it could be inferred that the excessive numerical dissipation error in the vorticity field is responsible for the overall discrepancy between the RANS solutions and measurements. It is difficult to accurately predict the tangential forces of the rotor blade using the LLM approach as single vortex element in the chordwise direction cannot sufficiently represent the three-dimensional geometry and various planform shapes of the rotor blades.

Comparing the averaged shaft torque and root flap-wise bending moment (RFBM) against the measured data are shown in Fig. 5. The NVLM results show that the predicted torque and RFBM are well-matched with the measurement for all yaw angles. It can be observed that their magnitude gradually decreases with increasing yaw angle as a result of a reduction in the axial flow velocity owing to yaw misalignment. It indicates that yaw inflow directly affects the global aerodynamic performance acting on the entire rotor system.

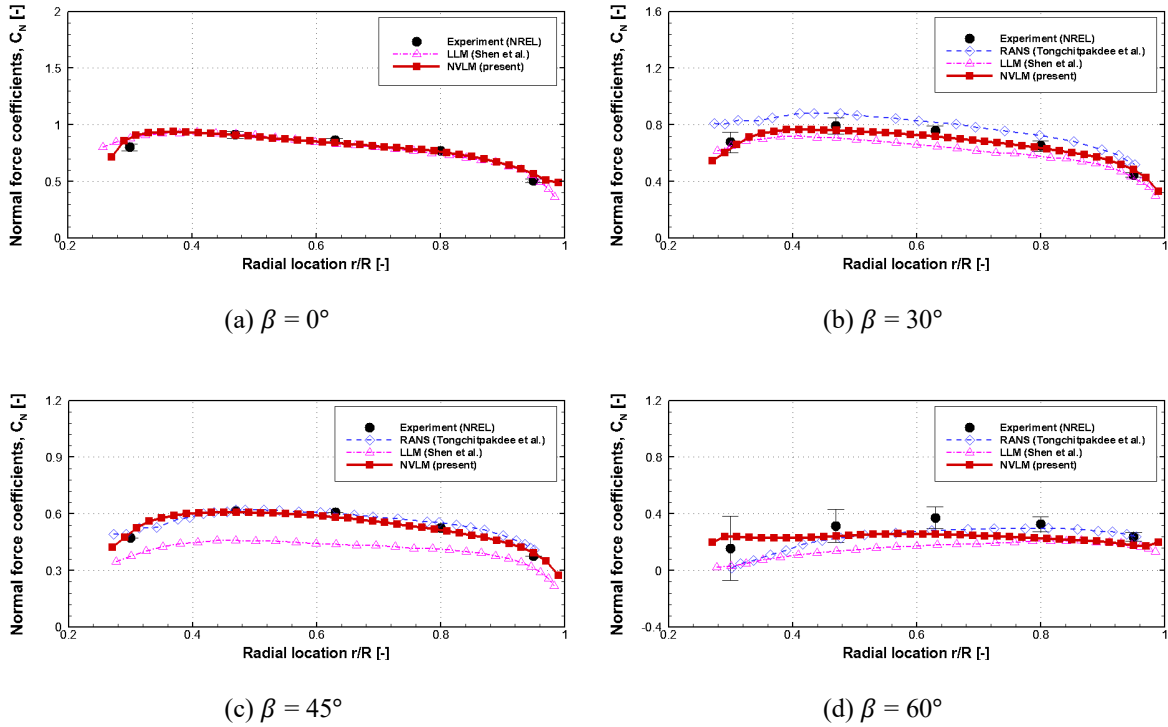


Fig. 3. Time-averaged normal force coefficients depending on yawing angles

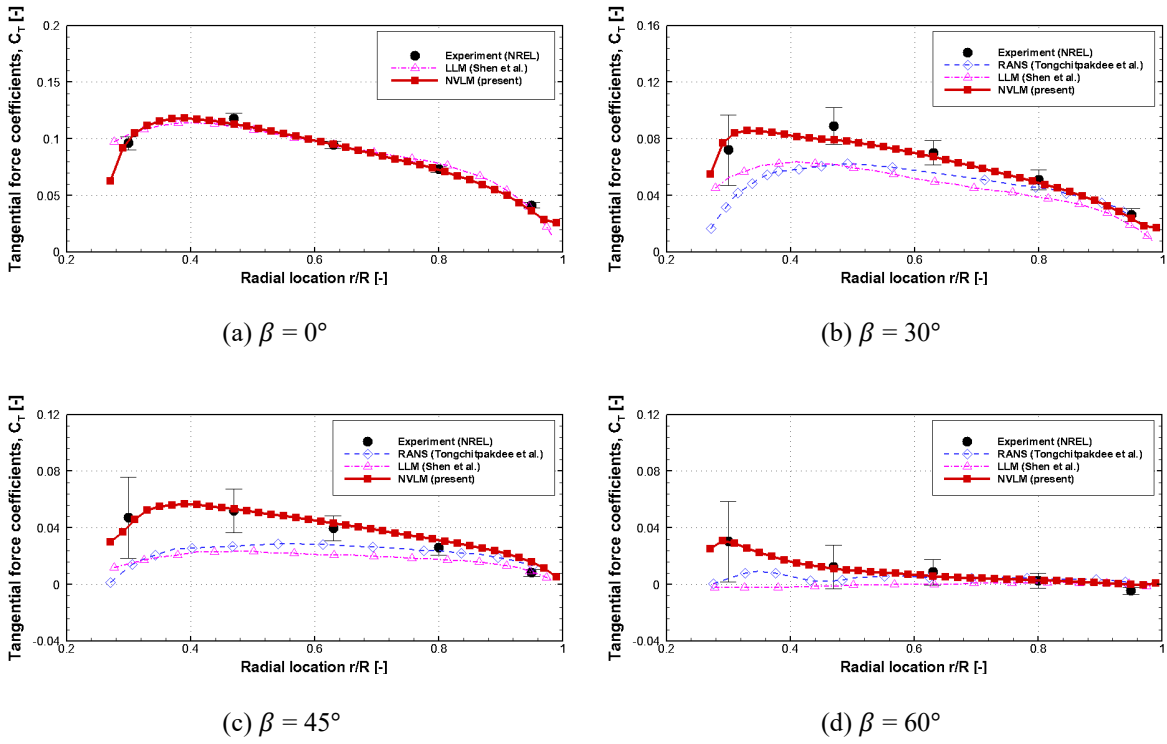


Fig. 4. Time-averaged tangential force coefficients depending on yawing angles

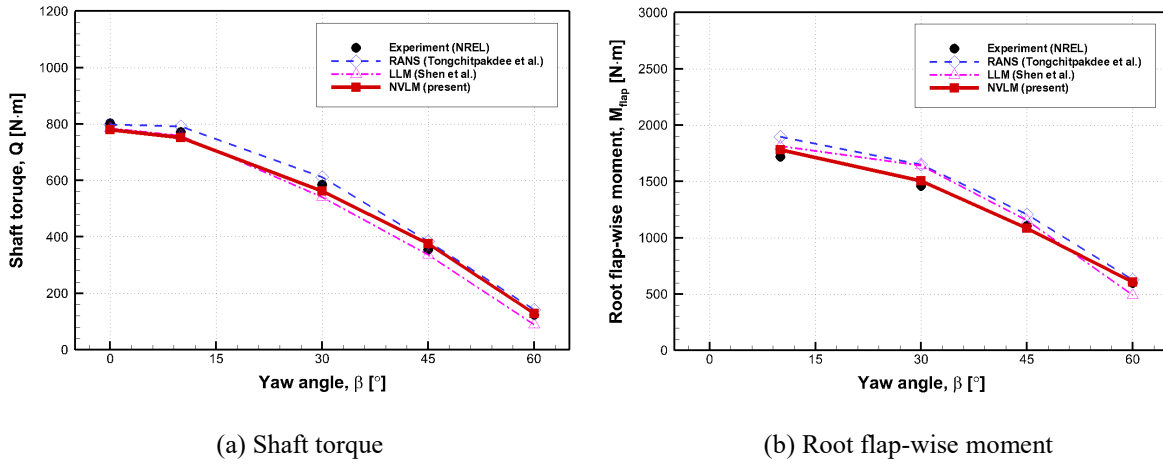
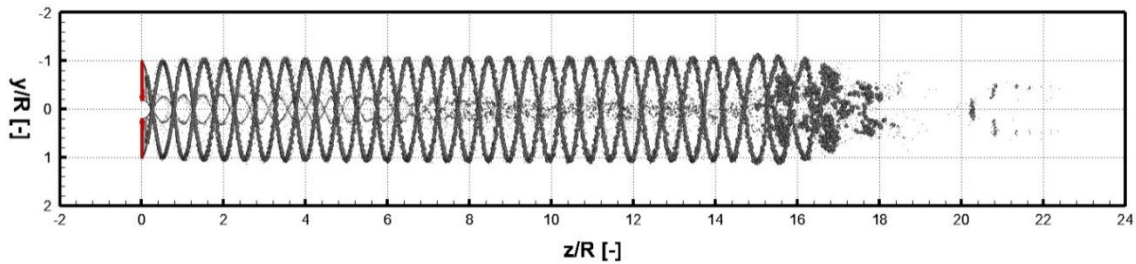


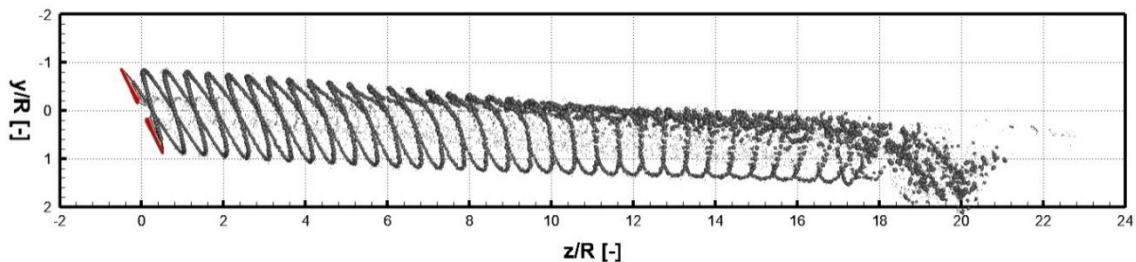
Fig. 5. Time-averaged shaft torque and root flap-wise moment depending on yawing angles

3.3 Evolution of skewed wake structures

In the present study, the wind turbine wake shed from the full span of the rotor blades was represented by vortex particles, rather than vortex filaments. Fig. 6 shows the developed wake geometries of wind turbine under axial and yawed flow conditions. The axisymmetric wake structure propagated downstream and its helical shape has remained up to 16 times of rotor radius for the non-yawed flow condition. It implies that the wake has evolved with azimuthally-symmetrical characteristics, except for far downstream where the initially generated wake during the slow rotation exists. On the contrary, it clearly appears as an asymmetrical wake structure for the yawed rotor configuration. Yaw misalignment leads to induced velocity and momentum in the spanwise direction (positive y-direction in Fig. 6 for positive yaw angle), and these are mainly responsible for deflecting the wake geometry towards the downwind side. Because of the skewed wake geometry, the wake behavior and propagation patterns became more unstable. Moreover, the helical wake structure has only remained up to about 6 times of rotor radius, after which it began to breakdown due to a strong interaction between tip and hub wake vortices. The downstream wake structure and flow field became extremely complex after the tip vortex breakdown phenomenon.



(a) $\beta = 0^\circ$



(b) $\beta = 30^\circ$

Fig. 6. Wake structure modeled by vortex particles depending on yawing angles (top view)

Fig. 7 and Fig. 8 show the vorticity contours in the z-direction at the different downstream locations and the streamwise (axial) velocity contour on the planes at the hub height of the wind turbine exposed to axial flow condition, respectively. The streamwise velocity contour is normalized using free stream velocity and the contour planes (x-y planes) are placed at $z/R = 4, 8, 12$ and 16 downstream. The contours also include the velocity vectors, which are associated with the velocity components in terms of the spanwise (radial) and tangential velocities. The symmetrical velocity deficit, with a circular wake flow around the rotor area, and vorticity fields can be clearly observed in Fig. 8.

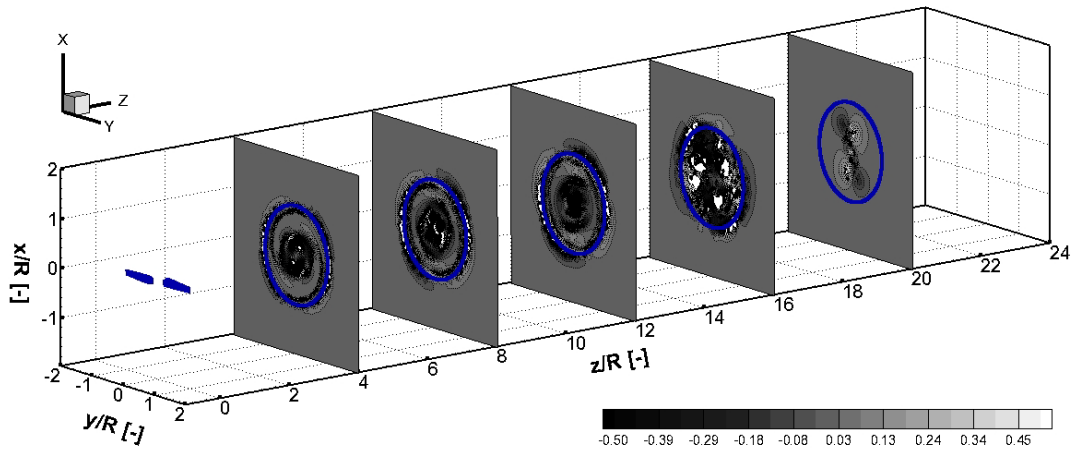


Fig. 7. Vorticity contours in the z-direction downstream at $\beta = 0^\circ$

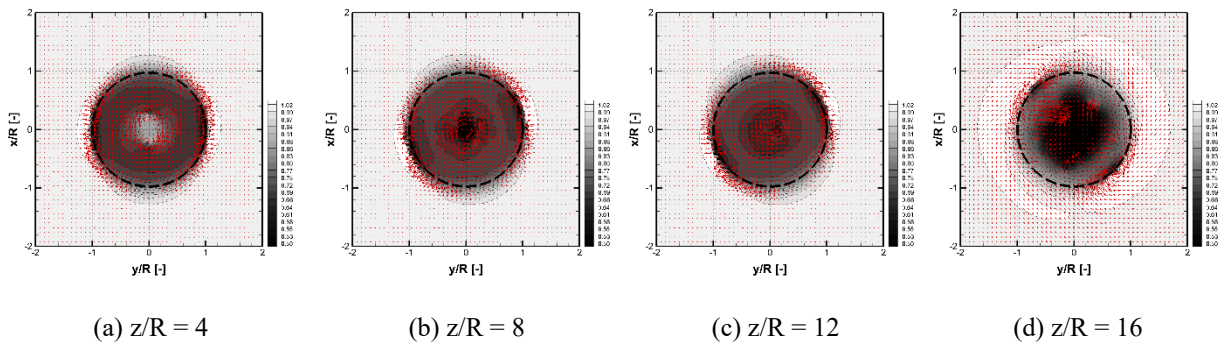


Fig. 8. Normalized streamwise (axial) velocity contour and velocity vector at $\beta = 0^\circ$

On the other hand, asymmetric vorticity and velocity fields were developed as a result of the skewed wake geometry, as can be seen in Fig. 9 and Fig. 10, respectively. The asymmetric vorticity field arising from the yawed-

rotor configuration yielded a highly complex flow field in the downstream. It is notable that the counter-rotating vortex pair were present at the top and bottom sides of the rotor area where the azimuth angles are 0° and 180° . Counter-rotating vortices were a major source of wake deflection toward the downwind side, and were responsible for the instability of wake propagation. Furthermore, a set of the counter rotating vortices transported the wake flow in the negative y -direction at the top and bottom edges of the rotor area, while they also developed a strong spanwise velocity component in the opposite direction (positive y -direction) at the center of the rotor area, as shown in Fig. 10. Consequently, counter-rotating vortex pair have a strong effect on the development of a curled velocity deficit, also referred to as a kidney-shaped velocity deficit [25]. Asymmetrically curled velocity deficit is much more pronounced and the wake shape dramatically deformed, as the wake evolved downstream. In a wind farm, if the upstream wind turbine is exposed to yawed flow, the skewed wake structure originating from the upstream wind turbine will play a crucial role in the determining of the inflow condition and aerodynamic performance of the subsequent wind turbines. Therefore, wake effects should be taken into account in order to evaluate an overall power output of a wind farm, and design its optimal layout.

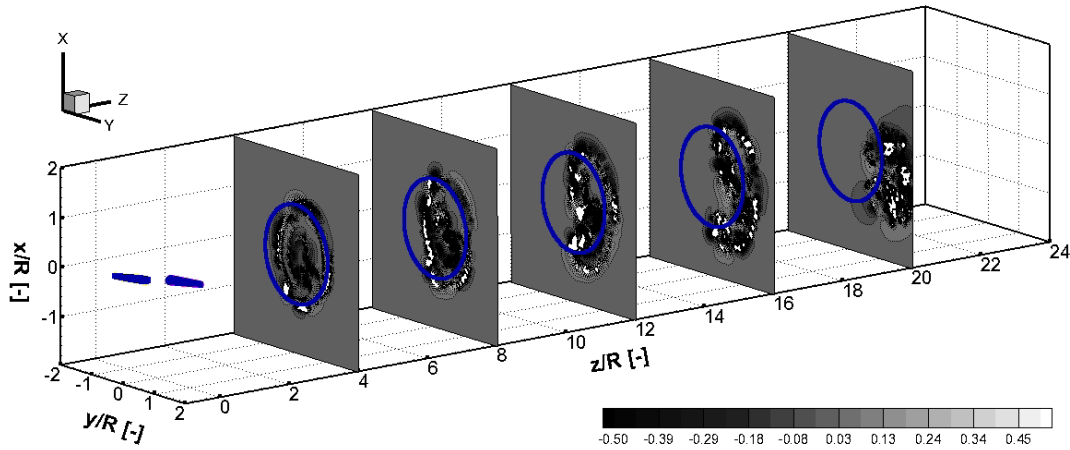


Fig. 9. Vorticity contours in the z -direction downstream at $\beta = 30^\circ$

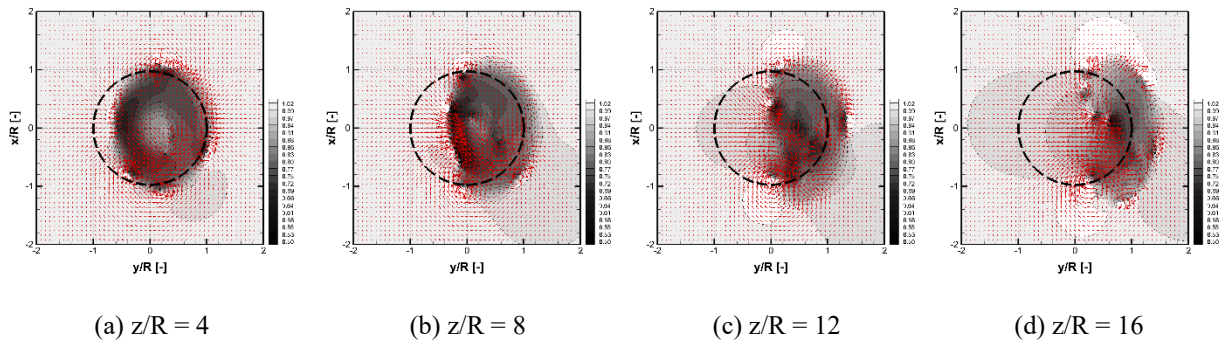


Fig. 10. Normalized streamwise (axial) velocity contour and velocity vector at $\beta = 30^\circ$

3.4 Effect of skewed wake structure

At yawed-rotor configuration under low wind speed conditions, the skewed wake effect becomes a dominant factor in determining the azimuthal aerodynamic loads as it leads to the variation in the axial induced velocity. Hence, investigating the impact of a non-axisymmetric wake on the unsteady aerodynamic behavior of the wind turbine blade is needed to accurately predict unsteady blade loading. Fig. 11 and Fig. 12 show the azimuthal distribution of axial velocity, the effective angle of attack on the rotor blade, and the thrust force at the axial and yawed flow conditions, respectively. It is noted that the effective angle of attack on the rotor blades does not exceed the stall onset angle of the S809 airfoil for all azimuth positions. Therefore, the flow conditions used in this study will not lead to the flow separation or dynamic stall phenomena. Stall delay model and dynamics stall model were not included when calculating the aerodynamic loads.

Under axial condition, the wind turbine wake was developed in a form of a helical geometry, and was transported downstream without the skewness, as already shown in Fig. 9. Helical wake structure leads to the azimuthally symmetric distribution of the wake-induced velocity and aerodynamic load as a function of only the radial position. On the contrary, a strong radial and azimuthal dependency on the axial velocity, effective angle of attack, and thrust force were clearly observed under yawed conditions, as depicted in Fig. 12. Under yawed conditions, the wake was deflected in the direction of the downwind side, thus resulting in a strong expansion downwind of the rotor and a weak expansion upwind of the rotor. Because of the skewed wake geometry, the distance between the trailing tip vortices and rotor plane is closer at the downwind side of the rotor blade ($\psi = 90^\circ$) compared to the upwind side ($\psi = 270^\circ$). The closer the trailing tip vortices are placed on the rotor plane, the larger the magnitude of the induced velocity normal

to the rotor plane is induced. Hence, the rotor blade on the downwind side experiences a smaller axial velocity and effective angle of attack than the rotor blade on the upwind side, leading to smaller load. Yawed rotor blades eventually suffer from the aerodynamic loading unbalance between the upwind and downwind sides of the rotor plane. For the outboard region, this consequently yields a restoring moment, referred to as a stabilizing moment. However, the opposite trend is obviously captured at the inboard region. A lower aerodynamic loading is found at the upwind side of the rotor blade compared to the downwind side. This is attributed to the root vorticity in the skewed wake and yields the destabilizing moment. It implies that the root vortices shed from the hub should be modeled to take into account the impact of the skewed wake structure on an asymmetric flow field and the unsteady aerodynamic behavior of the rotor blades, in particular, for low wind conditions. Yaw aerodynamics associated with a skewed wake effect were also confirmed in literature [6, 12].

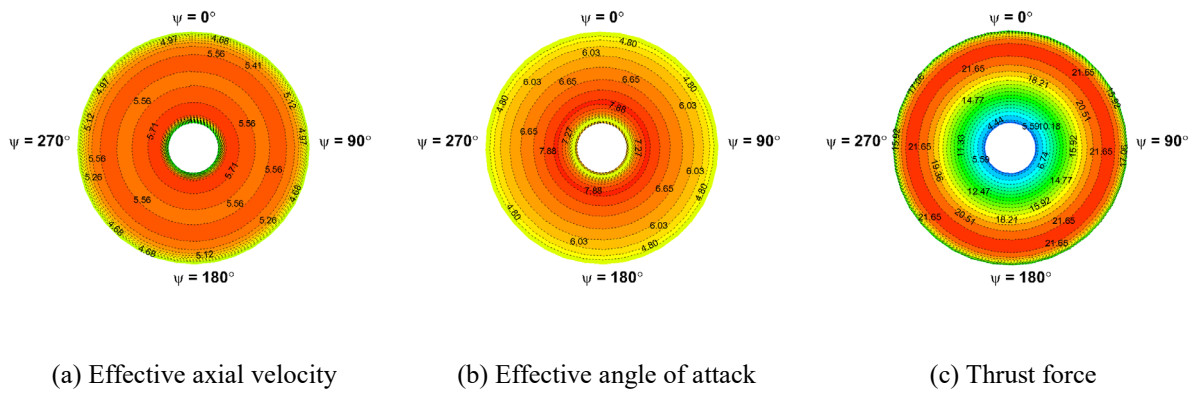


Fig. 11. Contours of effective axial velocity, effective angle of attack, and thrust force at $\beta = 0^\circ$

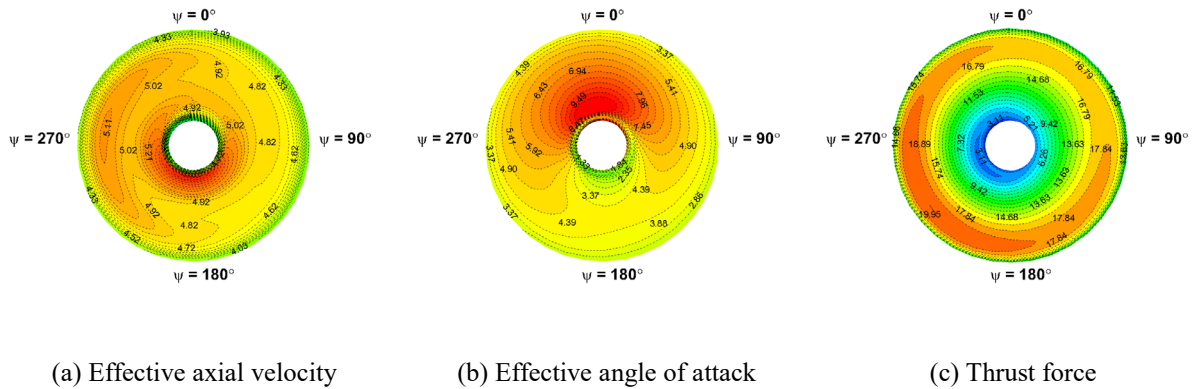


Fig. 12. Contours of effective axial velocity, effective angle of attack, and thrust force at $\beta = 30^\circ$

Yawed flow exerts an unsteady aerodynamic force on the rotor blade and introduces an azimuthal variation in the root flap-wise bending moment (RFBM) over a revolution, as illustrated in Fig 13. It is observed that the magnitude of the RFBM gradually decreases, while the amplitude of the fluctuation in the RFBM increases as the yawing angle increases. Time-dependent variations of the RFBM with different yawing angles have been converted to the frequency domain to find the frequency components of a periodic signal of the RFBM using a fast Fourier transform (FFT) method. Harmonics of the rotor rotational frequency corresponding to 1P, 2P, 3P, and so on, are captured, as shown in Fig. 14. Although only two harmonics corresponding to the blade passing frequency are observed at the yaw angle of 10° , several harmonics appear with increasing yaw angles. It indicates that a large yaw misalignment leads to a non-sinusoidal oscillation and nonlinear variation in the RFBM due to strong influences from the highly skewed wake structure behind the rotor. These could have a negative effect on the aeroelastic behavior and fatigue lifecycle of wind turbine blades.

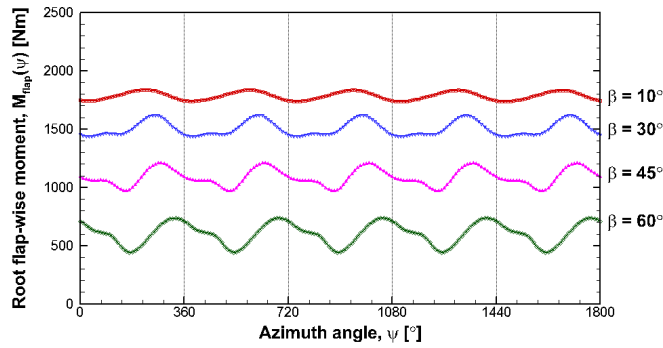


Fig. 13. Time history of root flap-wise moment depending on yawing angles

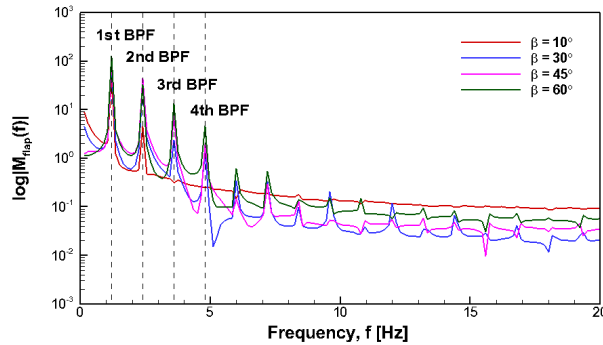


Fig. 14. Root flap-wise moment depending on yawing angles in frequency domain

4. Conclusion

In the present study, the impacts of the skewed wake on the unsteady aerodynamic behavior and performance of a wind turbine under yawed flow conditions were numerically investigated. For this purpose, the numerical simulation of the NREL Phase VI wind turbine model under yawed flow conditions was carried out using nonlinear vortex lattice method (NVLM) with vortex particle method (VPM), and predicted results were compared against the experiment. Comparison results showed that the NVLM predictions for the time-averaged normal and tangential loads, and overall aerodynamic performance of the wind turbine, were well-matched with the measurements, even for highly yawed flow conditions. It implies that the NVLM is capable of accurately predicting the cyclic variation in the induced velocity and unsteady aerodynamic behavior on the rotor blades caused by skewed wake geometry. It can also be observed that the rotor blades eventually experienced unbalanced loads between the upwind and downwind sides, thus incurring the stabilizing moment at the outboard sections and destabilizing moment at the inboard sections. Furthermore, a higher harmonic of the root flap-wise bending moment was clearly captured as the yaw angle increased, as non-sinusoidal oscillation and nonlinear variation behavior were more pronounced with increasing wake deflection angles. Under yawed flow condition, the wind turbine wake was deflected toward the downwind side of the rotor blade due to an induced cross-streamwise momentum. Skewed wake structure became considerably unstable and its geometry completely broke down as the wake propagated downstream due to the strong wake interaction between hub and tip vortices. A set of counter-rotating vortices placed at the top and bottom side of the rotor area was observed in the skewed wake structure. It turned out that counter-rotating vortex pair played a dominant role in the development of deflected wake geometry and asymmetrically curled velocity deficit. Discussion in the current work can help to acquire a better understanding of the unsteady wake characteristics and wake evolution mechanism.

The engineering models for correcting the airfoil data, such as the dynamic stall and stall delay models, can be applied to the NVLM. It is possible to take into account the dynamic stall effect and three-dimensional rotational effect, in particular, which are more predominant at the inboard section of the rotor blade. Hence, the numerical study on the yaw aerodynamics of a wind turbine using the NVLM can be extended to high wind speed conditions, where the advancing and retreating blade effect plays an important role in the variation in aerodynamic loads and flow behaviors around rotor blades. In addition, the transient wake behaviors, depending on the downstream position, can be captured. This provides a scope for further research to predict the overall power output and analyze the unsteady

wake dynamics of a wind farm where a great number of wind turbines will be installed in close proximity to each other.

Declaration of interest

There is no conflict of interest.

Acknowledgments

This research was supported by the Climate Change Research Hub of KAIST (Grant No. N11180110). This work was also supported by the Korea Institute of Energy Technology Evaluation and Planning (KETEP) and the Ministry of Trade, Industry & Energy (MOTIE) of the Republic of Korea (No. 20168520021200).

References

- [1] Fleming, P., Pieter, M.O.G., Lee, S., van Wingerden, J.W., Johnson, K., Churchfield, M., Michalakes, J., Spalart, P., and Moriarty, P., "Simulation comparison of wake mitigation control strategies for a two-turbine case," *Wind Energy*, 18(2), 2015, pp. 2135-2143.
- [2] Miao, W., Li, C., Yang, J., and Xie, X., "Numerical investigation of the yawed wake and its effects on the downstream wind turbine," *Journal of Renewable and Sustainable Energy*, 8, 2016, pp.03330.
- [3] Grant, I., Parkin, P., and Wang, X., "Optical vortex tracking studies of a horizontal axis wind turbine in yaw using laser-sheet, flow visualisation," *Experiments in Fluids*, 23(6), 1997, pp. 513-519.
- [4] Grant, I. and Parkin, P., "A DPIV study of the trailing vortex elements from the blades of a horizontal axis wind turbine in yaw," *Experiments in Fluids*, 28(4), 2000, pp. 368-376.
- [5] Vermeer, L.J., "A Review of Wind Turbine Wake Research at TU Delft," *20th ASME Wind Energy Symposium, 39th Aerospace Sciences Meeting and Exhibit*, AIAA-2001-0030, 2001.
- [6] Haans, W., Sant, T., van Kuik, G., and van Bussel, G., "Measurement of Tip Vortex Paths in the Wake of a HAWT Under Yawed Flow Conditions," *Journal of Solar Energy Engineering*, 127(4), 2005, pp. 456-463.

- [7] Bastankhah, M, and Porté-Agel, F., “A wind-tunnel investigation of wind-turbine wakes in yawed conditions,” *Journal of Physics: Conference Series*, 625, 2015, pp. 012014.
- [8] Bartl, J. and Sætran, L. “Blind test comparison of the performance and wake flow between two in-line wind turbines exposed to different turbulent inflow conditions,” *Wind Energy Science*, 2, 2017, pp. 55-76.
- [9] Howland, M.F., Bossuyt, J., Martínez-Tossas, L.A., Meyers, J., and Meneveau, C., “Wake structure in actuator disk models of wind turbines in yaw under uniform inflow condition,” *Journal of Renewable and Sustainable Energy*, 8, 2016, pp. 043301.
- [10] Schepers, J.G., Boorsma, K., Cho, T., Gomez-Iradi, S., Schaffarczyk, P., Jeromin, A., Shen, W.Z., Lutz, T., Meister, K., Stoevesandt, B., Schreck, S., Micallef, D., Pereira, R., Sant, T., Madsen, H.A., and Sørensen, N., “Final report of IEA Task 29, Mexnext (Phase 1): Analysis of Mexico wind tunnel measurements,” Technical Report, ECN-E12-004, Energy Research Center of the Netherlands, 2012.
- [11] Schepers, J.G., Boorsma, K., Gomez-Iradi, S., Schaffarczyk, P., Madsen, H.A., and Sørensen, N.N., Shen, W.Z., Lutz, T., Schulz, C., Herraéz, I. and Schreck, S., “Final report of IEA Wind Task 29: Mexnext (Phase 2), Technical Report, ECN-E—14-060, Energy Research Center of the Netherlands, 2014.
- [12] Schepers, J.G., “An Engineering Model For Yawed Conditions, Developed On Basis Of Wind Tunnel Measurements,” 37th Aerospace Sciences Meeting and Exhibit, AIAA-99-0039, 1999.
- [13] Ryu, K.W., Kang, S.H., Seo, Y.H., and Lee, W.R., “Prediction of Aerodynamic Loads for NREL Phase VI Wind Turbine Blade in Yawed Condition,” *International Journal of Aeronautical and Space Sciences*, 17(2), 2016, pp. 157-166.
- [14] Duque, E.P.N., Burklund, M.D., and Johnson, W., “Navier-Stokes and Comprehensive Analysis Performance Predictions of the NREL Phase VI Experiment,” *Journal of Solar Energy Engineering*, 125(4), 2003, pp. 457-467.
- [15] Shen, X., Zhu, X., and Du, Z., “Wind turbine aerodynamics and loads control in wind shear flow,” *Energy*, 36, 2011, pp. 1424-1434.
- [16] Tongchitpakdee, C., Benjanirat, S., and Sankar, L.N., “Numerical Simulation of the Aerodynamics of Horizontal Axis Wind Turbines under Yawed Flow Conditions,” *Journal of Solar Energy Engineering*, 127(4), 2005, pp. 464-474.
- [17] Yu, D.O., You, J.Y., and Kwon, O.J., “Numerical investigation of unsteady aerodynamics of a horizontal-axis wind turbine under yawed flow conditions,” *Wind Energy*, 16, 2013, pp.711-727.

- [18] Lee, H.J., and Lee, D.J., “Numerical investigation of the aerodynamics and wake structures of horizontal axis wind turbines by using nonlinear vortex lattice method,” *Renewable Energy*, 132, 2019, pp. 1121-1133.
- [19] Lee, H.J., Jo, Y.M., and Lee, D.J., “Development of Nonlinear Vortex Lattice Method and Its Application to Aerodynamic Analysis of Wind Turbine,” *6th Asian/Australian Rotorcraft Forum and Heli Japan*, 2017.
- [20] Lee, D.J., and Na, S.U., "Numerical simulations of wake structure generated by rotating blades using a time marching, free vortex blob method," *European Journal of Mechanics-B/Fluids*, 18(1), 1999, pp. 147–159.
- [21] Jang, J.S., Park, S.H., and Lee, D.J., "Prediction of Fuselage Surface Pressures in Rotor–Fuselage Interactions Using an Integral Solution of Poisson Equation," *Journal of the American Helicopter Society*, 59(4), 2014, pp. 1–11.
- [22] Park, S.H., Chu, Y.B., and Lee, D.J., “Investigation of Main Rotor-Tail Rotor Interaction in Hover Flight using Vortex Particle Method,” *5th Asian/Australian Rotorcraft Forum and 9th Australian Pacific Vertiflite Conference on Helicopter Technologies*, 2016.
- [23] Winckelmans, G.S. and Leonard, A., “Contributions to Vortex Particle Methods for the Computation of Three-Dimensional Incompressible Unsteady Flows,” *Journal of Computational Physics*, 109, 1993, pp. 247–273.
- [24] Hand, M.M., Simms, D.A., Fingersh, L.J., Jager, D.W., Cotrell, J.R., Schreck, S. and Larwood, S.M., “Unsteady Aerodynamics Experiment Phase VI: Wind Tunnel Test Configurations and Available Data Campaigns,” Technical Report, NREL/TP-500-29955, 2001
- [25] Schottler, J., Bartl J., Mühle F., Sætran L., Peinke J. and Hölling M., “Wind tunnel experiments on wind turbine wake in yaw: redefining the wake width,” *Wind Energy Science*, 3, 2018, pp. 257–273.